Tumor necrosis factor receptor-1-induced neuronal death by TRADD contributes to the pathogenesis of Japanese encephalitis

Vivek Swarup, Sulagna Das, Soumya Ghosh and Anirban Basu

National Brain Research Centre, Manesar, Haryana, India

Abstract

While a number of studies have documented the neurotropism of Japanese encephalitis virus (JEV), little is known regarding the molecular mechanism of neuronal death following viral infection. The tumor necrosis factor receptor (TNFR)-associated death domain (TRADD) has been suggested to be the crucial signal adaptor that mediates all intracellular responses from TNFR-1. Using mouse (Neuro2a) and human (SK-N-SH) neuroblastoma cell lines, we have shown that the altered expression of TNFR-1 and TRADD following JEV infection regulates the downstream apoptotic cascades. Activation of TRADD led to mitochondria-mediated neuronal apoptosis. As TRADD-knockout animals or deficient cell lines are unavailable, it has been difficult to definitively address the physiological role of TRADD in diseases pathology following JEV infection. We circumvented this problem by silencing TRADD expression with small-interfering RNA (*si*RNA) and have found that TRADD is required for TNFR-1-initiated neuronal apoptosis following *in vitro* infection with JEV. Interestingly, *si*RNA against TRADD also decreased the viral load in Neuro2a cells. Furthermore, *si*RNA against TRADD increased the survival of JEV-infected mice by altering the expression of pro apoptotic versus antiapoptotic molecules. These studies show that the engagement of TNFR-1 and TRADD following JEV infection plays a crucial role in neuronal apoptosis.

Keywords: apoptosis, caspase 3, mitochondria, neuron, tumor necrosis factor receptor 1, tumor necrosis factor receptor-associated death domain, virus.

J. Neurochem. (2007) **103**, 771–783.

Neuronal apoptosis is an essential process that contributes to the development of the nervous system and is thought to be regulated by a variety of physiological and non-physiological external stimuli. Among them, metabolic disturbances due to chemical insults and virus infections are conspicuous which can provoke apoptotic cell death. Several viral gene products affect apoptosis by interacting directly with components of the highly conserved biochemical pathway, which regulate neuronal apoptosis. On one hand, it appears that viruses block apoptosis to prevent premature death of the host cell and so maximize virus progeny from a lytic infection or facilitate a persistent infection. On the other hand, a growing number of viruses actively promote apoptosis. Thus it appears that viruses may perform both function, the latter being the culmination of a lytic infection and serving to spread virus progeny to neighboring cells, while evading host inflammatory response. Apoptosis may then contribute to the cytotoxicity associated with virus infection.

Flavivirus are important human pathogens causing variety of diseases ranging from mild febrile illness to severe encephalitis and hemorrhagic fever. Among them, Japanese encephalitis virus (JEV) that commonly affects children and is a major cause of acute encephalopathy (Chen *et al.* 2002). JEV is active over a vast geographic area that includes India, China, Japan, and virtually all of South-East Asia. In addition, JEV has been recently isolated from previously non-affected areas of Australia (Mackenzie *et al.* 2002). Approximately 3

billion people live in the JEV endemic area covering much of Asia with nearly 50 000 cases of Japanese encephalitis (JE) reported each year. Of these, about 10 000 cases results in fatality and a high proportion of survivors have serious neurological and psychiatric sequelae (Kaur and Vrati 2003). As JE viral replication occurs only in neurons, extensive neuronal loss is a hallmark of JEV-associated neurotropism (Yasui 2002). Pathological features of JEV-associated neurotropism include both microglia- and astroglia-related neuropathological complications (Ghoshal *et al.* 2007; Mishra *et al.* 2007). Unlike human immunodeficiency virus-associated neuronal loss which is generally thought not to be the result of direct viral infection of neurons, but rather due to the bystander damage caused by activated microglia/macrophages, JEV tends to cause neurotropic infection, infecting neural rather than non-neural cells in humans (Yang *et al.* 2004).

Despite the importance of CNS pathology in severity of disease progression, the mechanisms by which JEV and other encephalitic flaviviruses induce neuronal apoptosis remain largely unknown. *In vitro* studies have begun to elucidate the pathways involved in JEV-induced cell death. Caspase 3 is an effector caspase that function as a central regulator of apoptosis (Slee *et al.* 2001). JEV infection triggers apoptosis in different transformed cell lines, resulting in caspase 3 activation, cytochrome *c* release, and exposure of phosphatidylserine on the outer leaflet of the plasma membrane (Liao *et al.* 1997; Chen *et al.* 2006). Mouse embryonic stem cell-derived neurons and neuroblastoma cells rapidly undergo apoptosis within 2–3 days after JEV infection (Yang *et al.* 2004). Several other encephalitic flaviviruses also induce apoptosis: St Louis encephalitis virus triggered apoptosis in neuroblastoma cells (Parquet *et al.* 2002) and JEV induce apoptosis in cell lines via the endoplasmic reticulum stress pathway (Hase *et al.* 1990; Su *et al.* 2002). These results suggest that the initiation of programmed cell death may be a common feature of flavivirus replication. The cellular outcome of JEV replication depends on the interactions between host and viral factors. UV-inactivated JEV failed to induce cell death, suggesting that viral replication is required to trigger apoptosis (Lin *et al.* 2004).

The underlying mechanism of JEV-induced neuronal apoptosis is not fully understood. It has been demonstrated earlier that several members of the tumor necrosis factor receptor (TNFR) superfamily could induce cell death (Chen and Goeddel 2002). It had been also shown earlier that TNFR-1 has a conserved 'death domain' in the intracellular region, which is required for the major outcomes of tumor necrosis factor (TNF) induction, i.e. activation of caspases, cell death signaling, and nuclear factor κB activation (Hsu *et al.* 1996). It was also reported that the core protein of hepatitis C virus can promote cell death via TNF signaling pathways possibly as a result of its interaction with cytoplasmic tail of TNFR-1 (Zhu *et al.* 1998). These findings prompted us to examine whether TNFR-1-mediated cell death pathways play any role in JEV-mediated neuronal apoptosis.

In this study, we clearly demonstrate that JEV initiate neuronal death by activating TNFR-1 complex. This complex, which includes TNFR-associated death domain (TRADD), initiates the apoptotic cascade by activating p38 mitogen activated protein kinase (MAPK) and c-Jun N-Terminal Kinase (pJNK). We have also shown that neuronal apoptosis following JEV infection is mitochondria dependent. Recently, it was demonstrated that West Nile virus cause neuronal apoptosis via caspase 3-dependent pathway (Samuel *et al.* 2007). Likewise, we have found that JEV also causes caspase 3-dependent neuronal death. As TRADD initiates the apoptotic cascade, small-interfering RNA (*si*RNA) against TRADD inhibits JEV-induced neuronal death as well as reduce the mortality of animals following viral infection.

Materials and methods

Viruses and cell

The GP-78 strain of JEV was initially obtained from Dr Sudhanshu Vrati (National Institute of Immunology, New Delhi, India) and further propagated in suckling BALB/c mice. A 10% suspension of the brain tissue was made by homogenization in the Dulbecco's Modified Eagle's Medium (DMEM) followed by centrifugation at 10 000 *g* to remove cellular debris and filtered through 0.22-μm sterile filter (Millipore, Bedford, MA, USA). The mouse brain-derived virus was stored at $-70°C$ in small aliquots and was used as the source of virus for all the experiments (Appaiahgari *et al.* 2006). Mouse neuroblastoma cell line Neuro2a (N2a) was obtained from National Centre for Cell Science, Pune, India. Human neuroblastoma cell line SK-N-SH was a kind gift from Dr Kakoli Ghoshal, National Institute of Immunology, New Delhi. Both the cell lines were grown at 37°C in DMEM supplemented with 7.5% sodium bicarbonate (NaHCO$_3$), 10% fetal bovine serum, and penicillin/streptomycin. All the reagents related to cell culture were obtained from Sigma (St Louis, MO, USA) unless otherwise stated. JEV was titrated as described earlier (Appaiahgari *et al.* 2006).

Infection of Neuro2a and SK-N-SH cell lines with JEV

Neuro2a, mouse neuroblastoma cell line, was plated at 5×10^5 cells/well in a six well plate. After 24 h in DMEM with 10% serum, the cells were switched to serum-free media for 12 h. N2a cell line was then infected with either live JEV (multiplicity of infection [MOI] = 5) or mock-infected for 1 h. Similarly, SK-N-SH cells were plated and infected with live JEV. After adsorption, unbound viruses were removed by gentle washing with phosphate-buffered saline (PBS). Fresh serum-free medium was added to each well for further incubation. Cells were snap frozen at various time points (6–36 h with 6 h intervals between each time point) and were processed for immunoblot analysis as described later in Materials and methods.

Virus infection of animals

We have used a previously described animal model of JE with slight modification (Appaiahgari *et al.* 2006). Three- to 4-week-old BALB/

c mice of either sex were injected through tail-vein with $\sim 3 \times 10^5$ pfu (in 50 µL of PBS) of JEV of strain GP-78 and control animals received the same amount of PBS as the experimental group. Group of six mice were killed at each time point (3 and 6 days) either for tissue or protein. From third day post-infection, animals start showing symptoms of JE including limb paralysis, poor pain response, and whole body tremor. JEV-infected mice started dying on sixth day onwards till the ninth day when all the infected animals succumbed to infection. All experiments were performed according to the protocol approved by the Institutional Animal Ethics Committee.

Lactate dehydrogenase assay and trypan blue exclusion test

N2a cells were either mock-infected or JEV infected for 1 h and then kept at 37°C for time intervals starting at 6–42 h. Cell culture supernatants were assayed for CytoTox-ONE Homogeneous Membrane Integrity Assay (Promega Madison, WI, USA), a fluorimetric assay which depends on the levels of lactate dehydrogenase (LDH) released due to cell death (Krady *et al.* 2005). The assay was performed according to the manufacturer's protocol. Fluorescence was measured using a SpectraMAX Gemini EM (Molecular Devices, Sunnyvale, CA, USA) fluorescence plate reader at an excitation wavelength of 560 nm and an emission wavelength of 590 nm. Upon infection, viability of both the cell lines (N2a and SK-N-SH) was also documented using trypan blue exclusion test.

Immunohistochemistry

Animals at 3 and 6 days post-infection and age-matched controls used for immunohistochemistry were perfused with PBS containing 7 U/mL heparin, followed by a fixative containing 2.5% *p*-formaldehyde in PBS. The brains were processed for cryostat sectioning. Fluorescence immunohistochemistry was performed for the following antibodies: microglia/macrophages were labeled with rat anti-CD11b antibodies (1 : 100; BD Pharmingen, NJ, USA) and astrocytes were labeled with rat anti-glial fibrillary acidic protein (GFAP) antibodies (1 : 200; Sigma) which were then double stained with rabbit anti-TNFR-1 (1 : 50; Santa Cruz Biotechnology, Santa Cruz, CA, USA). The corresponding secondary antibodies were used: donkey anti-rabbit Alexa Fluor 594 (1 : 1000; Molecular Probes, Eugene, OR, USA) for CD11b and GFAP and goat anti-rabbit FITC (1 : 200; Vector Laboratories Inc., CA, USA) for TNFR-1. For mature neurons, NeuN staining was performed by antigen retrieval on the sections by incubating at 95°C in Na-citrate buffer (pH 6.0). The sections were then washed with 1X PBS and permeabilized using 6 N HCl for 8 min and subsequently treated with 0.1 mol/L Borax (pH 8.5) for 5 min. Sections were blocked for 1 h with blocking solution and then stained with mouse anti-NeuN (1 : 500; Chemicon, Temecula, CA, USA), incubated overnight at 4°C, which were then double stained with rabbit anti-TNFR-1. After 1X PBS wash, the sections were incubated in horse anti-mouse FITC (1 : 200; Vector Laboratories Inc.). The slides were mounted with Vectashield mounting media containing 4′6-diamidino-2-phenylindole (DAPI) (Vector Laboratories Inc.). The stained slides were observed under the Zeiss Axioplan 2 Fluorescence microscope (40× magnifications; Carl Zeiss, Thornwood, NY, USA).

Immunoblot analysis

The brain tissue from animals at 3 and 6 days post-infection and age-matched controls were dissected and placed in 1.5 mL microfuge tubes with 700 µL of freshly prepared 1X PBS, then lysed in lysis buffer containing 1% Triton X-100, 10 mmol/L Tris–HCl (pH 8.0), 150 mmol/L NaCl, 0.5% Nonidet P (NP-40), 1 mmol/L EDTA, 0.2% EGTA, 0.2% sodium *o*-vanadate, and protease inhibitor cocktail (Sigma). Samples were homogenized with teflon-glass homogenizer and centrifuged at 8000 *g* for 20 min. Supernatant was further sonicated and protein concentrations were determined using Bradford method.

N2a and SK-N-SH cells were washed twice with ice-cold 1X PBS and lysed in lysis buffer, DNA was sheared using a 24-gauge needle and the lysate was incubated on a rocking platform at 4°C for 30 min before centrifugation at 10 000 *g* for 15 min at 4°C. Protein concentrations were determined in the supernatant by Bradford method.

Ten micrograms of each sample was electrophoresed on a polyacrylamide gel and transferred onto a nitrocellulose membrane. The membrane was then blocked in 2.5% skimmed milk in 1X PBS–Tween-20 for 1 h at 25°C with gentle agitation. After blocking, the blots were incubated with rabbit anti-TNFR-1 diluted (1 : 1000; Santa Cruz) in 1% bovine serum albumin (BSA) for overnight at 4°C with gentle agitation. After extensive washes in 1X PBS-Tween-20, blots were incubated with goat anti-rabbit horseradish peroxidase (Vector Laboratories Inc.) at a dilution of 1 : 2500 in 1% BSA diluent for 1 h, with gentle agitation. The blots were rinsed again in 1X PBS–Tween-20. The chemiluminescence reagent from Roche (Basel, Switzerland) was used according to the manufacturer's instructions. The blots were developed by exposing them to Chemigenius, Bioimaging System (Syngene, Cambridge, UK). The images were captured and analyzed using the GeneSnap and GeneTools software (Syngene), respectively. The blots were stripped (30 min at 50°C in 62.5 mmol/L Tris–HCl pH 6.8, 2% sodium dodecyl sulfate, and 100 mmol/L 2-mercaptoethanol) and reprobed with anti-β-tubulin (1 : 2500; Sigma) to determine equivalent loading of samples. Similarly, blots were developed for anti-TNFR-1-associated factor (TRAF-2; 1 : 1000), anti-TRADD (1 : 1000), p53 (1 : 1000), Bax (1 : 1000), and Bcl-2 (1 : 1000). All these antibodies were purchased from Santa Cruz (Santa Cruz, CA, USA). Blots were also developed for anti-p38MAPK (1 : 1500), pASK-1 (1 : 1000), pJNK (1 : 1000), and cleaved poly (ADP-ribose) polymerase (PARP) (1 : 1500). These antibodies were purchased from Cell Signaling (Beverly, MA, USA). Appropriate secondary antibodies were used to develop the blots. Similarly, immunoblots from the time-kinetic experiment with mock-infected cells (N2a and SK-N-SH) were also developed using same antibodies mentioned previously.

RNA isolation and semi-quantitative RT-PCR analysis

Total cellular RNA was isolated from N2a cells or virus-infected and control animals as described previously (Basu *et al.* 2002). Isolated RNA was quantified using spectrophotometry, aliquoted, and stored at −70°C until further use. Reverse-transcriptase polymerase chain reaction (RT-PCR) was performed using the one-step RT-PCR kit (Qiagen Biosciences; Hamburg, Germany) following the manufacturer's protocol and reactions were carried out on Genius Techne thermal cycler (Jepson, Bolton, UK). Five hundred nanogram of the total RNA was used as template in 25 µL PCR reactions, containing 5X PCR Buffer (5 µL), dNTPs (1 µL), enzyme mix (1 µL), and specific forward and reverse primers (5 µmol/L) and RNase free

Table 1 Primers used for RT-PCR experiments and expected size of amplified products

	Forward primer	Reverse primer	Product size (bp)
TNFR-1	5′-CAGTCTGCAGGGAGTGTGAA-3′	5′-CACGCACTGGAAGTGTGTCT-3′	157
TRADD	5′-GGAGGATGAGCTCTGCAAAC-3′	5′-CAAACGTCTGCTGGTCTTGA-3′	157
GP-78	5′-TTGACAATCATGGCAAACGA-3′	5′-CCCAACTTGCGCTGAATAAT-3′	200
Cyclophilin	5′-CCATCGTGTCATCAAGGACTTCAT-3′	5′-TTGCCATCCAGCCAGGAGGTCT-3′	192

TNFR-1, tumor necrosis factor receptor-1; TRADD, tumor necrosis factor receptor-associated death domain; RT-PCR-reverse transcriptase-polymerase chain reaction.

water. Oligonucleotide primer pairs against mouse TNFR-1 and TRADD and cyclophilin mRNAs were chosen, checked for specificity using a basic local alignment and search tool (BLAST) search, and prepared from Sigma, Bangalore, India (Table 1). JEV (GP-78) envelope protein-specific primers were designed and checked for specificity using BLAST search (Table 1). PCR parameters were established for each primer set to determine the optimal annealing temperature and cycle number for evaluation within the linear range of amplification. Amplification of the mRNA sequences of TNFR-1, TRADD, GP-78, and cyclophilin produced single bands that were of the size predicted from the reported sequences for these mRNAs. PCR products were separated on 2% agarose gel, stained with ethidium bromide, and photographed using GeneSnap software provided with Chemigenius Bioimaging System, Syngene. Photographs were analyzed by GeneTools software provided with same Bioimaging system.

Active caspase 3 assay
Mock or JEV-infected N2a cells were sonicated on ice in 100 μL of lysis buffer. The Colorimetric CaspACE Assay System was purchased from Promega and used according to the manufacturer's directions for the 96-well plate assay format. Duplicate assays were performed for each sample, with blanks and mock-infected. Following the user's instructions, the absorbance was measured at 405 nm in Biorad Microplate reader (Biorad, Hercules, CA, USA). Caspase 3 enzyme activity was expressed as picomoles of caspase 3 liberated per milligram of protein per minute (Krady *et al.* 2005).

Measurement of mitochondrial cytochrome *c* release
To study the release of cytochrome *c*, N2a cells were either mock infected or JEV infected (MOI 1 : 5). Mitochondrial fraction was isolated and following the user's protocol (Sigma) the cytochrome *c* assay was performed. The absorbance was measured at 550 nm in Biorad Microplate reader.

RNA interference
To selectively prevent TRADD expression, we employed the RNA interference technology. A double-stranded RNA (*si*RNA) was employed to degrade TRADD mRNA and thus to limit the available TRADD protein. The *si*RNA experiments were designed and conducted as described earlier (Baker-Herman *et al.* 2004). The *si*RNAs directed against the TRADD mRNA (NM_001033161) consisted of sequences with symmetrical 3′-UU overhangs using *si*STRIKE™ U6 Hairpin Cloning RNA Inteference Systems (Promega, Madison, WI, USA). The sequences were designed and validated by using the *si*RNA Target Designer Algorithm (Promega) and were submitted to a BLAST search to avoid the possible

targeting of other homologous genes. The sequence of the most effective TRADD *si*RNAs represented is as follows: 5′-GAAGAG-CGCUGUUUGAAUU-3′, 5′-CUUCUCG CGACAAACUUAA-3′. To account for the non-sequence-specific effects, scrambled Non-Targeting *si*Mock-infected cell was used. The sequence of scrambled *si*RNA is as follows: 5′-GUGCACAU GAGUGAGAUUU3′ and 5′-CACGUGUACUCACUCUAAA-3′. This also comprised non-targeting *si*RNAs with comparable GC content to that of the functional *si*RNA but lacks identity with known gene targets which was confirmed by BLAST analysis to have at least four mismatches with all known human, mouse, and rat genes. *si*RNA sequences were manufactured by Proligo, Singapore. TRADD *si*RNAs or the scrambled *si*RNAs were suspended in diethyl pyro-carbonate water to yield desired concentration. For *in vitro* transfection, cells were plated in 24-well plates and transfected with 0.6 μmol/L *si*RNAs with 10 μL lipofectamine (Invitrogen, Carlsbad, CA, USA). The cells were then kept for 72 h in OptiMEM medium (Gibco, Rockville, MD, USA). After 72 h, cells were infected with JEV for 1 h and kept in serum-free media for 36 h. Total RNA or proteins were then collected from these samples and analyzed.

TUNEL assay
Mouse neuroblastoma cell N2a and human neuroblastoma cell SK-N-SH were plated at a density of 5×10^4 cells/well of eight well chamber slides (Nunc, Denmark) in medium containing 10% fetal bovine serum. After 24 h, the cells were transfected with TRADD *si*RNA using lipofectamine in some of the conditions. After 72 h of transfection, the cells were either mock infected or JEV infected for 1 h and kept for 24 h. Apoptotic cells were identified using *In situ* Cell Death Detection Kit, tetramethyl rhodamine red (Roche, Germany). Briefly, the cells were fixed with 4% *p*-formaldehyde in 1X PBS and blocked with 4% BSA containing 0.02% Triton X-100. The fixed cells were then incubated in the TUNEL mix (terminal deoxynucleotidyl transferase in storage buffer and tetramethyl rhodamine red labeled-nucleotide mixture in reaction buffer) for 1 h at 25°C (Maggirwar *et al.* 1999). The slides were mounted with Vectashield mounting media containing DAPI.

Measurement of mitochondrial membrane potential
N2a cells were plated in 60-mm tissue culture plate at subconfluent density. Twenty-four hours later, cells were either *si*RNA transfected or infected with JEV (MOI 1 : 5) or both. Later, the cells were incubated with 5 μmol/L JC-1 fluorescence dye (Molecular Probes) for 30 min in the CO_2 incubator and washed several times with PBS pre-warmed at 37°C. Mitochondrial membrane potential was evaluated qualitatively under a Zeiss Axioplan 2 Fluorescence microscope (20× magnifications) using 568 nm filter (Dikshit *et al.* 2006).

Evaluation of siRNA administration in JEV-infected animal

For *in vivo* experiment, the *si*RNAs were suspended in 1X PBS to yield a concentration of 50 μmol/L, and 17 μL of *si*RNA-PBS mix was combined with 3 μL of oligofectamine and incubated at 25°C for 20 min. The TRADD or the scrambled *si*RNAs and PBS were slowly injected in 3-week-old BALB/c mice intracerebrally (Basu *et al.* 2002; Kang *et al.* 2006; Satriotomo *et al.* 2006). After 2 h, mice were either injected with PBS or infected with 3×10^5 pfu of lethal dose of JEV through tail vein. Following viral infection, all four groups of animal [(PBS injected control, JEV infected, scramble *si*RNA + JEV infected (sc-JEV), and TRADD *si*RNA + JEV infected (si-JEV)] were observed for survival. After 6–7 days following *si*RNA injection and subsequent JEV infection representative animals from each group were killed for the isolation of protein. Immunoblots were performed for TRADD, Bax, and Bcl-2 and active Caspase 3 was measured as described earlier in Materials and methods section.

Statistical analysis

The data are expressed as mean ± SEM. Comparisons among groups were performed by one-way ANOVA followed by Bonferroni multiple comparisons post-test.

Results

JEV induces neuronal cell death

Neurotropism of JEV was assessed by evaluating the time course of neuronal death using N2a cell line. Briefly, N2a cells were either mock or live JEV infected for 1 h. After a brief wash with PBS, the cells were kept in serum-free media for various time points starting from 6 to 42 h, cytotoxicity measured at regular intervals of 6 h. Cells were then assayed for LDH as a measurement of cell death. The fluorometric measurement of the assay was expressed as percent cytotoxicity. There was a graded increase in the cytotoxicity in JEV-infected samples when compared with mock-infected samples (Fig. 1a). The percentage cytotoxicity was significantly increased at 6 h after JEV infection (twofold increase over control, $p < 0.001$), with the cytotoxicity reaching closely to 92% in 36–42 h following JEV infection (4.5-fold increase, $p < 0.001$).

We also performed trypan blue exclusion test using both N2a and SK-N-SH cell lines. In both the cell lines, cell death was significantly increased at 6 h after JEV infection (twofold increase over mock infected, $p < 0.01$), with the death increasing to about 90% in 36–42 h following JEV infection (about 4.5-fold increase over mock infected, $p < 0.001$) (Fig. 1b).

JEV induces over-expression of TNFR-1 complex

The TNFR-l-associated proteins involved in generating the various TNF-α-induced signals are TRAF-2 and TRADD, a novel protein that interacts specifically with the death domain of TNFR-l. TNFR-1 activation promotes binding of TRADD and subsequent recruitment of TRAF-2 to promote apoptosis. The expression of key molecules associated with TNFR-1
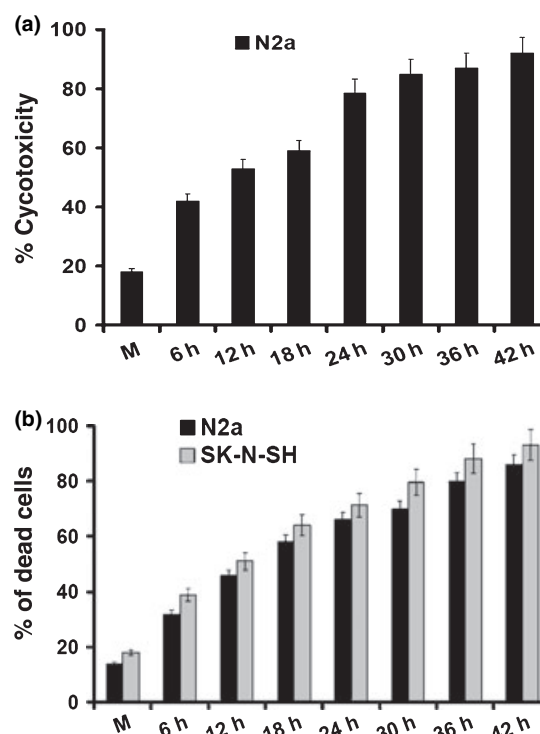
Fig. 1 JEV induces neuronal apoptosis in mouse and human neuroblastoma cells. (a) Mouse N2a cells were either mock infected or JEV infected for 1 h and then kept at 37°C for 6–42 h. Cell culture supernatants were assayed for lactate dehydrogenase. Data represent mean ± SEM from three independent experiments. (b) Trypan blue exclusion test was performed on both mouse N2a and human SK-N-SH cells. Cell counting was performed using Leica microscope and represented as bar graph. Data represent mean ± SEM from three independent experiments.

complex at various time points was determined by immunoblot analysis. The expression of TNFR-1 increased gradually from 6 h post-infection, reaching its highest levels at 12 h (4.5-fold increase over corresponding mock infected, $p < 0.01$) and decreasing steadily thereafter. Similar pattern was noticed for TRAF-2, which increased three- and fourfolds over the corresponding mock infected ($p < 0.001$) at 12 and 18 h, respectively. However, the level of TRAF-2 was drastically reduced post-18 h JEV infection. The twofold increase in TRADD levels over corresponding mock infected observed at 18 h, remained at the same level till 36 h (Fig. 2a). While TNFR-1 over-expression was seen in N2a cells infected with JEV, we did not observe the same in microglial cell line BV2 indicating that the over-expression is specific to neuronal cells (*data not shown*).

To further confirm this hypothesis, we also investigated the protein levels in human neuroblastoma cells, SK-N-SH, following JEV infection. The levels of TNFR-1 increased significantly (fourfold increase over corresponding mock infected, $p < 0.001$) at 12 h post-infection. We have observed similar trends for TRAF-2, which increased approximately
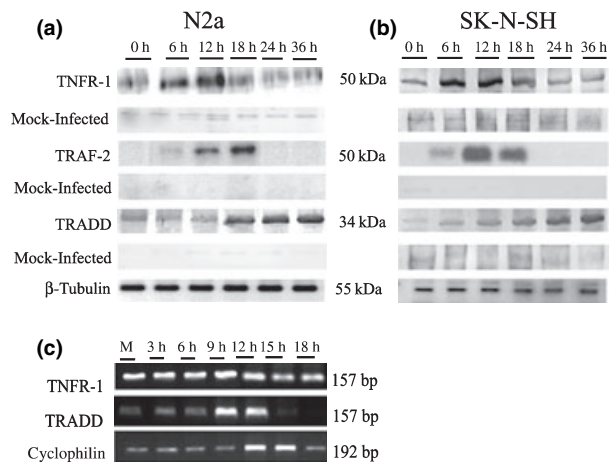
Fig. 2 JEV infection induces over-expression of tumor necrosis factor receptor-1 and associated complex. N2a cells were infected with either live JEV (multiplicity of infection = 5) or mock infected for 1 h. After adsorption, unbound viruses were removed by gentle washing with phosphate-buffered saline, and cells were further incubated in fresh serum-free medium. Mock- and virus-infected cells were snap frozen at various time points (as indicated) and were processed for immunoblot analysis. (a) Blots were developed against tumor necrosis factor receptor 1 (TNFR-1), TNFR-1-associated factor (TRAF-2), and TNFR-associated death domain (TRADD). Data shown is a representative of three individual experiments. (b) Similar experiment was performed with SK-N-SH cells. Protein samples were isolated and blots were developed for TNFR-1, TRAF-2, and TRADD. In both the cell lines, a distinct increase in TNFR-1, TRAF-2, and TRADD levels was observed in JEV-infected samples. (c) Total mRNA was isolated from mock-infected and JEV-infected N2a cells at various time points as indicated and reverse transcribed. The levels of TNFR-1 and TRADD assessed using semi-quantitative RT-PCR.

sixfold at 12 h. The 2.5-fold increase in TRADD expression over corresponding mock infected at 18 h post-infection was further elevated to fourfold at 36 h. (Fig. 2b).

We further investigated the mRNA transcripts levels of TNFR-1 and TRADD in mock-infected and JEV-infected cells at various time points (3, 6, 9, 12, 15, and 18 h). The significant ($p < 0.01$) twofold increase in TNFR-1 mRNA observed at 3 and 6 h post-infection was down-regulated at later time points, with transcripts reaching levels comparable with that of mock-infected control. Similar trend was observed with TRADD levels, with mRNA levels elevated significantly by twofold ($p < 0.001$) at 6 and 9 h when compared with the mock-infected control (Fig. 2c).

TNFR-1 over-expression induces ASK-1-p38MAPK/ pJNK cascade

The expression levels of key signaling molecules associated with TNFR-1-mediated cell death like pASK-1, p38MAPK, pJNK, and p53 was determined in JEV-infected N2a cells by immunoblot. The level of pASK-1 and p38MAPK was elevated by greater than three- and fivefold, respectively, at

36 h post-infection when compared with the corresponding mock-infected control ($p < 0.001$). As increased reactive oxygen species levels has been implicated in the JEV-infected N2a cells (Mishra *et al.* 2007) and as elevated levels of reactive oxygen species causes increased pJNK activation (Yoshizumi *et al.* 2000; Kamata *et al.* 2005), we determined the levels of pJNK in JEV-infected N2a cells. A significant ($p < 0.001$) 11-fold increase in pJNK was observed in JEV-infected N2a after 30–36 h, when compared with mock-infected samples. A gradual time-dependent increase in p53 level was also observed in JEV-infected N2a cells (Fig. 3a and b).

JEV infection induces mitochondrial-dependent neuronal apoptosis by modulating pro- and antiapoptotic molecules

As pJNK mediates the release of proapoptotic protein cytochrome *c* from mitochondria (Ohtsuka *et al.* 2003) and as pJNK was elevated following JEV infection, we evaluated
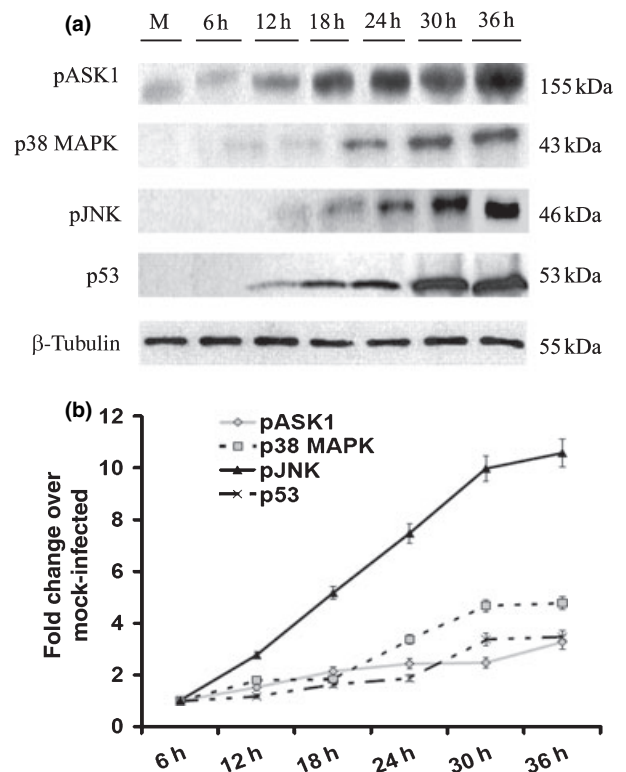

Fig. 3 JEV induces pASK-1-p38MAPK/pJNK cascade. Proteins from mock and JEV-infected N2a samples were subjected to immunoblot analysis. (a) Blots were developed using antibodies against pASK-1, p38MAPK, pJNK and p53. Data shown is a representation of three different experiments. The blots were stripped and reprobed with β-tubulin to confirm equal protein loading. (b) Densitometric analysis of the blots showing activation of pASK-1 and other downstream molecules. Data represents fold changes over corresponding mock-infected samples at different time points (immunoblots from the mock-infected samples are not shown). Data represent mean ± SEM from three independent experiments.

the effect of JEV infection on mitochondrial membrane integrity. JEV infection of N2a cells resulted in disruption of mitochondria as evident from increased release of cytochrome c. A gradual increase in the specific activity of cytochrome c oxidase was observed with increased time post-infection (6–72 h). A significant three-, six-, and 7.5-fold increase in cytochrome c activity was observed at 12, 36 and 72 h, respectively, when compared with mock-infected control (Fig. 4a).

The expression level of Bcl-2, an antiapoptotic protein is tightly regulated with the changes in mitochondrial membrane integrity. A gradual decrease in Bcl-2 expression was accompanied by a concurrent increase in the expression of pro-apoptotic protein Bax. A twofold decrease in Bcl-2 levels and twofold increase in Bax expression were observed at 36 h post-infection, when compared with mock-infected samples (Fig. 4b and c).

As activation of caspase 3 is a hallmark of apoptosis, we evaluated the amount of active Caspase 3 in N2a cells following viral infection. To quantitatively examine the kinetics of JEV-induced caspase 3 activation, mock-infected and JEV-infected samples were assayed by a substrate-specific caspase 3 activity assay. The fivefold increase (over mock infected, $p < 0.001$) in caspase 3 activity observed at 18 h post-infection was gradually elevated over time with Caspase 3 activity increased to 20-fold over mock infected at 48 h post-infection (Fig. 4d).

Moreover, Caspase 3 cleaves PARP, an event which ultimately leads to DNA fragmentation and apoptosis (Boulares *et al.* 1999). Infection of N2a cells with JEV for 30–36 h, resulted in a significant ($p < 0.001$) threefold increase in the levels of cleaved PARP when compared with mock-infected N2a cells (Fig. 4b and c).

Induction of TNFR-1-associated apoptotic signal inducing molecules in JEV-infected mice

Tissue samples from control- and JEV-infected animals brain were analyzed for the expression of TNFR-1 and associated
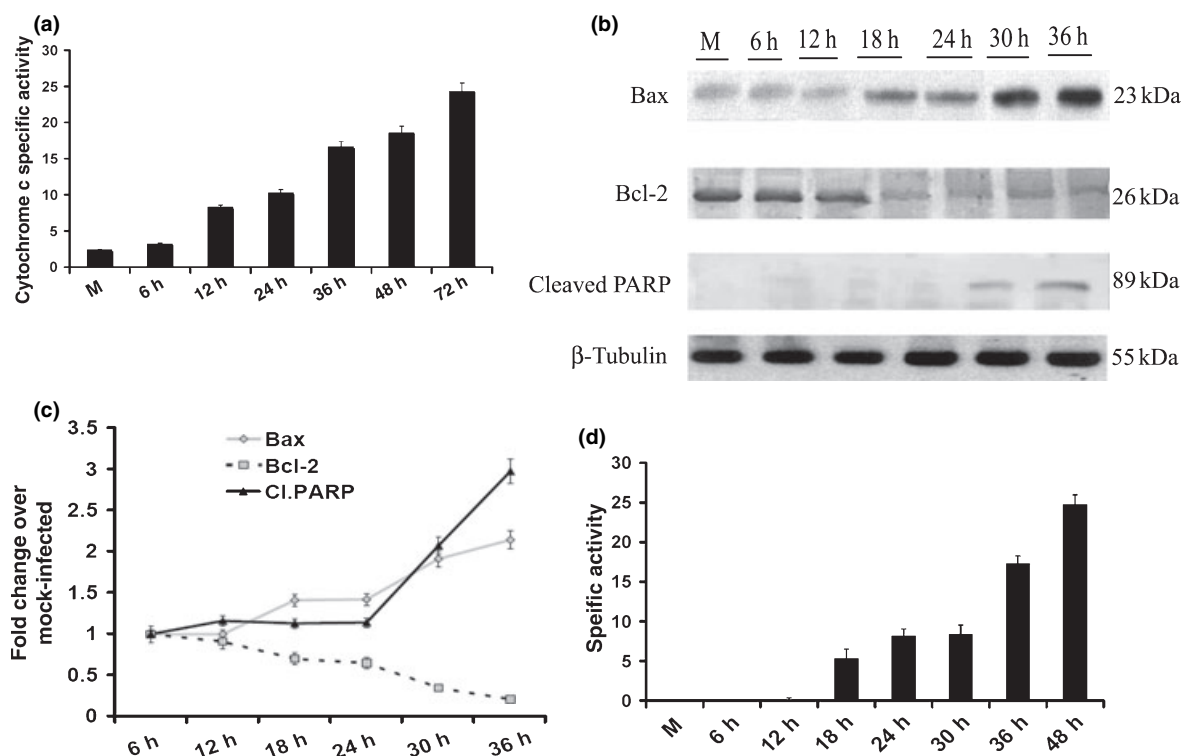

Fig. 4 JEV infection induces mitochondria-dependent neuronal apoptosis by modulating pro and antiapoptotic molecules. (a) Mitochondrial fraction was isolated from mock- and JEV-infected N2a cells. The isolated fraction was assayed for cytochrome c. Data represent mean ± SEM from three independent experiments. (b) Proteins from mock and JEV-infected N2a samples were subjected to immunoblot analysis. Blots were developed using antibodies against Bcl-2, Bax, and cleaved poly (ADP-ribose) polymerase (PARP). The blots were stripped and reprobed with β-tubulin to confirm equal protein loading. Data shown here is a representation of three different experiments. (c) Densitometric analysis (fold changes over mock-infected samples at different time points) of the blots showing expression levels of Bax, Bcl-2, and cleaved PARP. The blots from the mock-infected samples were not shown. Data represent mean ± SEM from three independent experiments. (d) Protein lysates were analyzed for caspase 3-specific activity. Caspase 3 enzyme activity was expressed as picomoles of caspase 3 liberated per milligram of protein per minute. Data represent mean ± SEM from three independent experiments.

molecules. A significant ($p < 0.01$) 2- and 1.8-fold increase in TNFR-1 and TRADD expression, respectively, over control was observed in 3 day infected mice (Fig. 5a and b). This increase in expression was followed by a decrease in TNFR-1 and TRADD level in 6 day infected mice, with levels remaining comparable with that of control. To identify the source of TNFR-1, immunohistochemistry was performed on brains sections obtained from control and JEV-infected animals. The double staining of TNFR-1 with NeuN (a marker for neuron) in the infected brain was clearly evident (Fig. 5d-inset), but no such double-positive cells were observed in brain sections obtained from control animal (*data not shown*). Co-localization of TNFR-1 and CD11b (a marker for microglia/macrophage) or TNFR-1 and GFAP (a marker for astrocytes) was not observed (Fig. 5e and f). Thus over-expression of TNFR-1 complex following JEV infection is limited only to the cells of neuronal lineage and not in others.

We next evaluated the expression of downstream mediators of TNFR-1-associated apoptosis, in control and JEV-infected mice. The levels of p38MAPK and pJNK was significantly ($p < 0.01$) up-regulated by 2.2- and 2-fold over control, respectively, in 3 days infected animals. This was followed by a reduction in expression at 6 days post-infection with levels of p38MAPK and pJNK being comparable with control animals (Fig. 5a and b). Since active JNK phosphorylates Bcl-2 to reduce its half-life (Maundrell *et al.* 1997), levels of Bcl-2 was down-regulated in 3 days (1.6-fold decrease over control) when compared with control and 6 days infected mice. Conversely, 2.3- ($p < 0.05$) and 2.5- ($p < 0.001$) fold increase in Bax levels over control was observed in tissue isolated from the brain of 3 and 6 days infected mice, respectively (Fig. 5a and c).

TRADD *si*RNA decreases the level of JEV-specific mRNA transcript in infected neurons

We next investigated whether *si*RNA against TRADD would decrease the TRADD-specific mRNA and protein in N2a cells. *si*RNA transfected and JEV-infected cells (denoted as si*-JEV) had reduced levels of TRADD-specific mRNA and
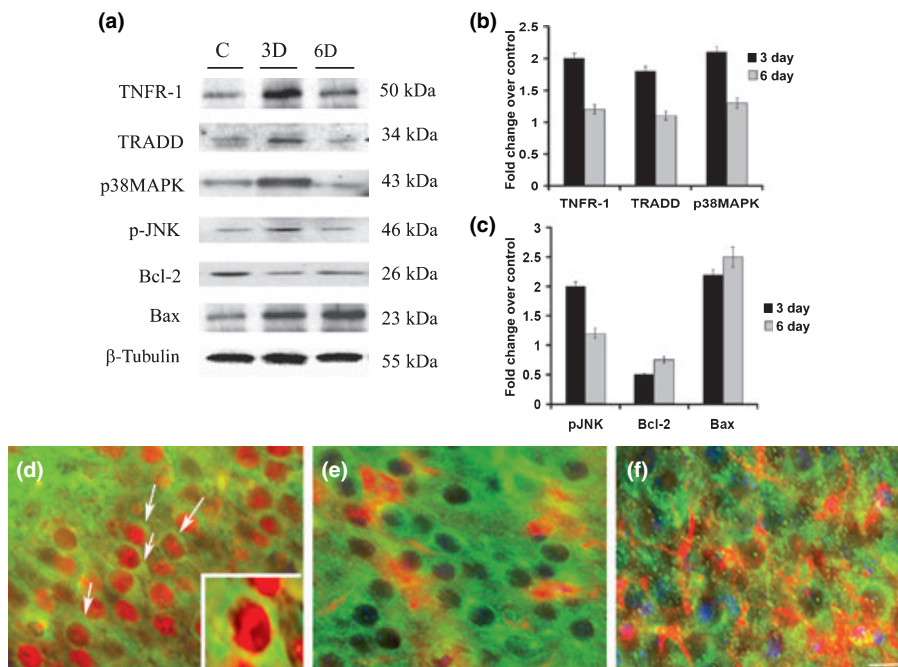

Fig. 5 *In vivo* JEV infection initiates tumor necrosis factor receptor 1 (TNFR-1) -mediated apoptotic pathway. Protein isolated from BALB/c mice brains [control (phosphate-buffered saline injected), 3 and 6 days post-infected] were analyzed by immunoblot. (a) A significant increase in the level of TNFR-1, TNFR-associated death domain (TRADD), p38MAPK, and pJNK at 3 days post-infection was followed by a decrease at 6 days post-infection. Bcl-2 levels were reduced and Bax levels were increased in infected mice. Data shown is a representative of six individual animals from each group. The blots were stripped and reprobed with β-tubulin to confirm equal protein loading. (b and c) The graph represents the fold changes over control in the expression levels of various proteins in infected animals. Data represent the mean-s ± SEM from six animals in each group. Cryostat sections from control and 3 days post-infected BALB/c mice brain were double-stained for TNFR-1 and NeuN (for neurons; d), or CD11b (microglia; e), and GFAP (astrocytes; f) and mounted using Vectashield containing DAPI. The 3 days infected mice had neurons over-expressing TNFR-1 as indicated by TNFR-1 and NeuN double positive cells (*co-localization shown by arrows*). However, neither microglia nor astrocytes over-expressed TNFR-1. The control brain showed negligible presence of TNFR-1 over-expressing cells (*data not shown*) (40× magnification). The inset in (d) shows the high power magnification of cells co-expressing TNFR-1 and NeuN.

protein, when compared with cells infected with JEV alone. A sixfold reduction in TRADD mRNA (Fig. 6a) and fivefold reduction in TRADD protein (Fig. 6b) were observed in si*-JEV when compared with JEV infected (without *si*RNA transfection) samples ($p < 0.001$).

We also evaluated the effect of TRADD down-regulation on the viral load in JEV-infected N2a cells. GP-78-specific primers were used to document the expression level of GP-78-specific mRNA transcripts. We found that GP-78 mRNA transcript levels were reduced to about 3.5-folds ($p < 0.001$) in si*-JEV than in JEV-infected cells (without any transfection) (Fig. 6c).

TRADD *si*RNA reduced neuronal apoptosis

We hypothesized that the decrease in TRADD protein should affect the apoptotic signal induced by JEV. We subjected si*-JEV cells to TUNEL assay and counted the percentage of TUNEL-positive cells (*graphical representation not shown*). While JEV-infected samples had significant TUNEL-positive cells (marker for apoptotic nuclei), the number of TUNEL-positive cells reduced drastically (twofold decrease than JEV-infected sample, $p < 0.01$) in si*-JEV samples (Fig. 7a–d). The results obtained from TUNEL assay clearly indicate that TRADD *si*RNA protect N2a cells from JEV-induced apoptosis. Similarly, *si*RNA knockdown experiments were performed in human SK-N-SH cells. Negligible cell death was observed when SK-N-SH was mock infected (Fig. 7i) or transfected with *si*RNA alone (Fig. 7j). A significant increase in TUNEL-positive cells was observed in JEV-infected samples (Fig. 7k), while significantly less number of TUN-EL-positive cells was observed in si*-JEV group (Fig. 7l).

TRADD *si*RNA reduces apoptosis via mitochondrial-dependent mechanism

We further investigated the mechanism behind the observed reduction in cell death in si*-JEV samples. As, JEV infection induces mitochondrial-dependent apoptosis; we elucidated the role of mitochondrial potential in *si*RNA-transfected samples, using the cationic dye JC-1 that signals the loss of

mitochondrial potential in apoptotic cells. Apoptotic cells can be identified by a decrease in JC-1 red fluorescence and an increase in JC-1 green fluorescence in the cytoplasm. The mock-infected and *si*RNA transfected N2a cells had predominant red fluorescence (Fig. 7e and f, respectively). JEV-infected cells had disrupted mitochondrial potential as indicated by increased green fluorescence (Fig. 7g). However, transfection with TRADD *si*RNA before JEV infection in N2a cells reduced the damage of mitochondrial integrity as shown by reduced green fluorescence than JEV-infected samples (without transfection with *si*RNA) (Fig. 7h). This result suggests that TRADD *si*RNA rescues JEV-infected N2a cells from apoptosis by preserving mitochondrial integrity.

TRADD siRNA increases survival of JEV-infected mice

We next evaluated the effect of TRADD *si*RNA in an experimental model of JE. Three-week-old mice were injected intracerebrally with either TRADD *si*RNA or scrambled *si*RNA and after 2 h, mice were either injected with PBS or infected with JEV. The mice were observed for the progression of the disease. Animals infected with JEV alone showed symptoms within 3 days of infection and all the animals succumbed to infection within 8–9 days. Scrambled *si*RNA conferred no protection to the animal with the time course of disease progression remaining similar to those infected with JEV alone. On the other hand, 80% of the TRADD *si*RNA pre-injected and JEV-infected mice survived for a longer period of time ($p < 0.01$) without any significant outcome of the behavior associated with disease progression (Fig. 8a; *data not shown for behavioral studies*).

Not only did transfection with TRADD *si*RNA confer protection to animal from JEV infection, it also altered the levels of proapoptotic molecules Bax (2.5-fold decrease than JEV infected, $p < 0.01$) and antiapoptotic molecule, Bcl-2 (twofold increase than JEV infected, $p < 0.01$) (Fig. 8b). TRADD level was itself significantly reduced in *si*RNA-injected and JEV-infected group when compared with JEV infected alone or scrambled *si*RNA-injected and
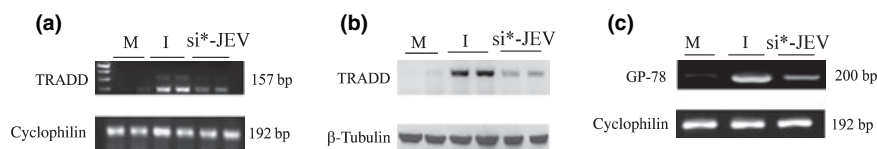

Fig. 6 TNFR-associated death domain (TRADD) small-interfering RNA reduces JEV-specific viral mRNA transcript. M, mock infected; I, JEV infected; si*-JEV, transfected with TRADD small-interfering RNA + JEV infected. (a) Total RNA were isolated from the mock infected or JEV infected or TRADD si-RNA and JEV infected (denoted as si*-JEV) N2a cells. The levels of TRADD were assessed using semi-quantitative RT-PCR and quantified using the GeneTools software. Each condition comprises of two different samples. There was a significant reduction in TRADD levels in si*-JEV samples when compared with JEV-infected samples. (b) Total protein were isolated from the mock infected or JEV infected or TRADD si-RNA and JEV-infected (denoted as si*-JEV) N2a cells and were subjected to immunoblot analysis using an antibody against TRADD. A significant decrease in the protein TRADD level in si*-JEV samples was observed. (c) The level of GP-78-specific mRNA transcripts was assessed in the RNA samples isolated from three different groups mentioned earlier (a). A significant reduction in GP-78-specific mRNA transcript level was observed in si*-JEV samples. Cyclophilin was used as an internal control.
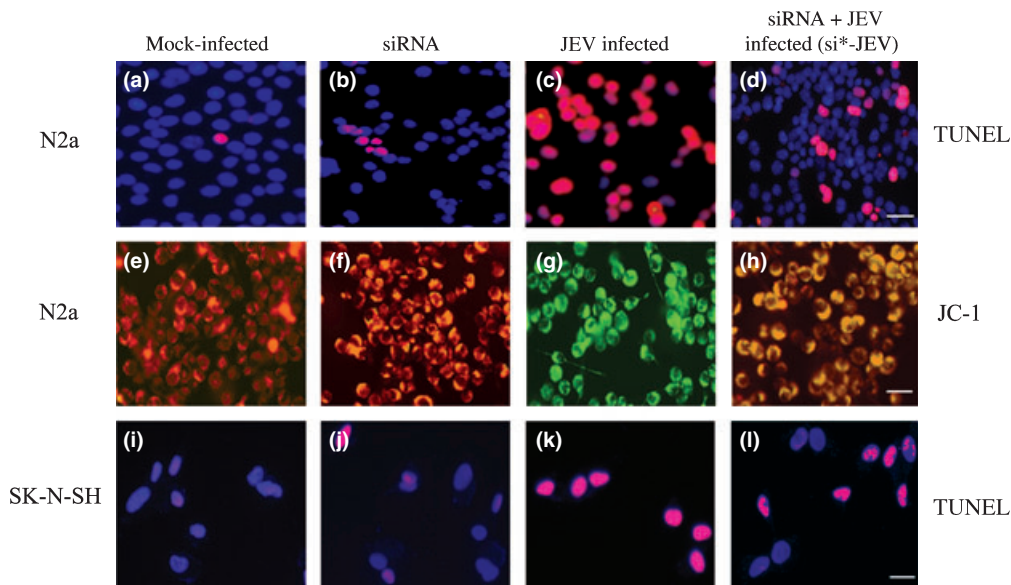
Fig. 7 Silencing with TNFR-associated death domain (TRADD) small-interfering RNA (*si*RNA) reduces JEV-induced neuronal apoptosis. N2a cells were either untransfected or transfected with TRADD *si*RNA for 72 h. After 72 h, the cells were either mock infected or infected with live JEV for 1 h and TUNEL was performed. The figure shows TUNEL-positive cells (red) co-localized with DAPI. Negligible cell death was observed when N2a cells were mock infected (a) or only transfected with TRADD *si*RNA (b). A significant increase in TUNEL-positive cells in JEV-infected cells was noticed (c). On the other hand, a significant reduction in TUNEL-positive cells was observed in *si*RNA transfected and JEV infected (si*-JEV) cells (d; 40× magnification). (e–h) N2a cells were either untransfected or TRADD *si*RNA transfected for 72 h. After 72 h, the cells were either mock or JEV infected for 1 h. The cells were then incubated with JC-1 fluorochrome and the images were captured.

The shift of red fluorescence to diffuse green shows disruption of membrane potential. While mock-infected (e) or only *si*RNA trans-fected (f) cells have predominantly red fluorescence; there was a significant increase in green fluorescence which was observed in JEV-infected samples (g). si*-JEV-infected cells with significantly reduced green fluorescence, indicates reduced mitochondrial membrane damage (h; 40× magnification). (i–l) SK-N-SH cells were either un-transfected or transfected with TRADD *si*RNA for 72 h. After 72 h, the cells were either mock-infected or infected with live JEV and TUNEL assay was performed. Negligible cell death was observed in mock-infected SK-N-SH cells (i) or only *si*RNA transfected (j). However, there was a significant increase in the TUNEL-positive cells in JEV-infected samples (k). si*-JEV-infected cells have significantly reduced TUNEL-positive cells (l; 40× magnification).

JEV-infected group (threefold than JEV infected, $p < 0.001$). si-JEV mice also had significantly reduced levels of Caspase 3 when compared with only JEV-infected or sc-JEV group (twofold decrease than JEV-infected samples, $p < 0.01$) (Fig. 8c). Thus, *in vivo* studies clearly demonstrated the prevention of apoptotic cascade and increased survivability in si-JEV mice.

Discussion

The induction of cell death is an essential part of normal life itself. Cell death control has been adapted to a variety of physiological needs, particularly in complex organisms. Among the numerous mechanisms for cell death signaling prevalent, one fascinating mechanism of cell death signaling is initiated by interaction of members of the TNF ligand family with their cellular receptors (Ashkenazi and Dixit 1998).

The present study was designed to examine the ability of TRADD to initiate the process of neuronal apoptosis follow-

ing JE. To this end, we used a mouse neuroblastoma N2a, which present many of the phenotypic properties of mouse primary neurons. We have shown previously that N2a are susceptible to cell death (i) following JEV infection (Mishra *et al.* 2007) and (ii) by neurotoxins released by activated microglia following JEV infection (Ghoshal *et al.* 2007). In the present communication, we have shown that *in vitro* virus infection (i) modulates the induction of TNFR-1-associated proteins (TNFR-1, TRAF-2, and TRADD) in N2a cell in time-dependent fashion, (ii) up-regulates several signaling molecules (pASK-1, p38 MAPK, pJNK, and p53) which directly regulate apoptosis, and (iii) modulates the induction of pro- and antiapoptotic molecules (Bax, Bcl-2, cleaved PARP, and caspase 3). We have further shown that *si*RNA against TRADD inhibit neuronal apoptosis following JEV infection. Using an *in vivo* model of JE, we have also showed that (i) TNFR-1 is expressed predominantly in neurons, but not in microglia or in astrocytes, (ii) there is a modulation of anti- and proapoptotic proteins and signaling molecules which are related to cell death, and (iii) administration of
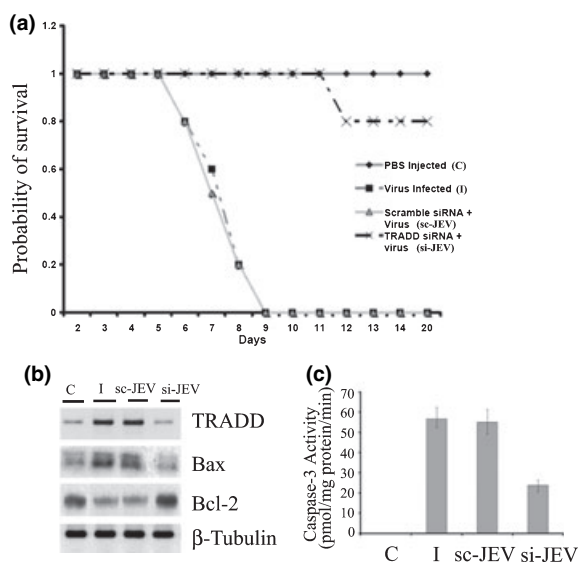
Fig. 8 TNFR-associated death domain (TRADD) small-interfering RNA (*si*RNA) injection *in vivo* significantly increases the survival of JEV infected mice. C, phosphate-buffered saline injected; I, JEV infected; sc-JEV, scrambled *si*RNA pre-injected and JEV infected; si-JEV, TRADD *si*RNA pre-injected and JEV infected. Three-week-old BALB/c mice were injected either with scrambled *si*RNA or TRADD *si*RNA intra-cerebrally. After 2 h, the mice were either phosphate-buffered saline-injected or JEV infected (3×10^5 pfu) through tail vein. (a) The survival of the mice groups was expressed as a graph. JEV-infected mice start dying on sixth day onwards till the ninth day when all the JEV-infected animals succumbed to infection. Scrambled *si*R-NA conferred no protection to the animals. On the other hand, 80% of TRADD *si*RNA injected mice survived for a longer period of time ($p < 0.01$), $n = 10$ for each group. (b) Protein samples isolated from the brains of animals were analyzed for TRADD, Bcl-2, and Bax levels. The TRADD and Bax levels were significantly decreased and Bcl-2 level was significantly up-regulated in si-JEV mice. Data shown here is a representative of six individual animals from each group. (c) Protein lysates were analyzed for caspase 3-specific activity and expressed as picomoles of caspase 3 liberated per milligram of protein per minute. si-JEV mice had significantly reduced levels of Caspase 3 when compared with only JEV infected or sc-JEV group. Data represent mean ± SEM of six animals from each group.

TRADD *si*RNA increases the rate of survival in animal. We have also showed that SK-N-SH, a human neuroblastoma is also susceptible to JEV induce neuronal apoptosis, and transfection with *si*RNA against TRADD confers protection from virus-induced apoptosis.

It has been well established that the cytoplasmic region of TNFR-1 interacts with a number of cellular proteins, which are components of the TNFR-1-mediated signaling complex. At least four such proteins have been identified; receptor interacting protein and TRAF-2 are responsible for TNF-induced pJNK or nuclear factor κB activation (Hsu *et al.* 1995; Liu *et al.* 1996), while fas associated death domain (FADD) and TRADD can induce apoptosis (Chinnaiyan *et al.* 1995; Hsu *et al.* 1996). These proteins bind either directly or

indirectly to the death domain or its vicinity in TNFR-1. JEV therefore may potentially disrupt or enhance these interactions and result in alterations of TNFR-1 signaling. TNFR-1-dependent apoptotic cell death of JEV-infected neurons could be a protective or pathologic host response. Apoptosis can act as an innate defense that restricts viral spread by eliminating infected cells and triggering pathogen recognition pathways. Alternatively, cell death could directly contribute to the spread and replication of JEV in CNS microenvironment. Like the hepatitis C virus core protein, it is possible that the proteins from JEV also bind to the death domain of TNFR-1, thereby, potentially disrupting or enhancing these interactions to alter TNFR-1 signaling (Zhu *et al.* 1998).

Several other TNFR-1-binding factors revealed altered expression in JEV-infected samples. TRAF-2, which binds TRADD and promotes pJNK activation via apoptosis signaling kinase (ASK-1), was also decreased in both *in vitro* and *in vivo* JEV samples. TNFR-1 over-expression has been known to induce variety of molecular events closely associated with apoptotic events. Of these the activation of the ubiquitously expressed ASK-1 and MAP3K are critical. Binding of ASK-1 to the adaptor protein TRAF-2, results in displacement of an inhibitory intermolecular interaction between the two molecules, allowing activation of ASK-1. ASK-1 is known to induce apoptosis by regulating stress-activated protein kinase kinase 1/mitogen activated protein kinase kinase (MKK)4-JNK and MKK3/6-p38 MAPK (Ichijo *et al.* 1997). Constitutively, active ASK-1 over-expression has been shown to cause apoptosis through mitochondrial-dependent caspase activation (Hatai *et al.* 2000). Thus, ASK-1 appears to be a key player in the MAPK (p38 MAPK/pJNK) induced cell death pathway (Sarker *et al.* 2003). Increased TNFR-1 expression in JEV samples suggests receptor involvement in cell death. However, not all TNF-α signaling factors are affected, because FADD expression levels remained unchanged in protein isolated from JEV-infected brain tissues (*data not shown*). It is noteworthy that both receptors (FADD and TRADD) have a death domain in their intracellular cytoplasmic region, which is responsible for the induction of apoptosis. Apoptosis was reduced by antisense depletion of TRADD expression (Zheng *et al.* 2006). TRADD expression is therefore required for JEV-induced neuronal apoptosis.

Tumor necrosis factor receptor-associated death domain is a crucial signal adaptor that mediates all intracellular responses from TNFR-1. As TRADD-deficient animal model is unavailable, we circumvented this problem by silencing TRADD expression with *si*RNA. We found that TRADD is required for TNFR-1 to induce neuronal apoptosis and diseases progression following JE. JEV initiates a TNFR-1-induced TRADD-mediated neuronal apoptosis by regulating complex signaling cascades which involves several anti- and proapoptotic molecules. Our finding clearly indicates that following JEV infection in animal TNFR-1 is predominantly

expressed in neuron not in microglia or astrocytes, this result prompt us to conclude that TNFR-1 is critical for neuronal apoptosis following JE.

Our experiments suggest that the expression of TNFR-1 in neurons changes following JEV infection and it initiate the death cascades via TRADD. The finding appears to offer one of the novel explanations of neurotropism in JEV. Obviously, more research is required to determine how JEV infection initiates TNFR-1- and TRADD-mediated neuronal apoptosis and subsequent progressive neurodegeneration.

Acknowledgements

References

Appaiahgari M. B., Saini M., Rauthan M., Jyoti and Vrati S. (2006) Immunization with recombinant adenovirus synthesizing the secretory form of Japanese encephalitis virus envelope protein protects adenovirus-exposed mice against lethal encephalitis. *Microbes Infect.* **8**, 92–104.

Ashkenazi A. and Dixit V. M. (1998) Death receptors: signaling and modulation. *Science* **281**, 1305–1308.

Baker-Herman T. L., Fuller D. D., Bavis R. W., Zabka A. G., Golder F. J., Doperalski N. J., Johnson R. A., Watters J. J. and Mitchell G. S. (2004) BDNF is necessary and sufficient for spinal respiratory plasticity following intermittent hypoxia. *Nat. Neurosci.* **7**, 48–55.

Basu A., Krady J. K., O'Malley M., Styren S. D., DeKosky S. T. and Levison S. W. (2002) The type 1 interleukin-1 receptor is essential for the efficient activation of microglia and the induction of multiple proinflammatory mediators in response to brain injury. *J. Neurosci.* **22**, 6071–6082.

Boulares A. H., Yakovlev A. G., Ivanova V., Stoica B. A., Wang G., Iyer S. and Smulson M. (1999) Role of poly(ADP-ribose) polymerase (PARP) cleavage in apoptosis. Caspase 3-resistant PARP mutant increases rates of apoptosis in transfected cells. *J. Biol. Chem.* **274**, 22932–22940.

Chen G. and Goeddel D. V. (2002) TNF-R1 signaling: a beautiful pathway. *Science* **296**, 1634–1635.

Chen C. J., Raung S. L., Kuo M. D. and Wang Y. M. (2002) Suppression of Japanese encephalitis virus infection by non-steroidal anti-inflammatory drugs. *J. Gen. Virol.* **83**, 1897–1905.

Chen S. O., Chang T. J., Stone G., Chen C. H. and Liu J. J. (2006) Programmed cell death induced by Japanese encephalitis virus YL vaccine strain or its recombinant envelope protein in varied cultured cells. *Intervirology* **49**, 346–351.

Chinnaiyan A. M., O'Rourke K., Tewari M. and Dixit V. M. (1995) FADD, a novel death domain-containing protein, interacts with the death domain of Fas and initiates apoptosis. *Cell* **81**, 505–512.

Dikshit P., Chatterjee M., Goswami A., Mishra A. and Jana N. R. (2006) Aspirin induces apoptosis through the inhibition of proteasome function. *J. Biol. Chem.* **281**, 29228–29235.

Ghoshal A., Das S., Ghosh S., Mishra M. K., Sharma V., Koli P., Sen E. and Basu A. (2007) Proinflammatory mediators released by activated microglia induces neuronal death in Japanese encephalitis. *Glia* **55**, 483–496.

Hase T., Summers P. L. and Dubois D. R. (1990) Ultrastructural changes of mouse brain neurons infected with Japanese encephalitis virus. *Int. J. Exp. Pathol.* **71**, 493–505.

Hatai T., Matsuzawa A., Inoshita S., Mochida Y., Kuroda T., Sakamaki K., Kuida K., Yonehara S., Ichijo H. and Takeda K. (2000) Execution of apoptosis signal-regulating kinase 1 (ASK1)-induced apoptosis by the mitochondria-dependent caspase activation. *J. Biol. Chem.* **275**, 26576–26581.

Hsu H., Xiong J. and Goeddel D. V. (1995) The TNF receptor 1-associated protein TRADD signals cell death and NF-kappa B activation. *Cell* **81**, 495–504.

Hsu H., Shu H. B., Pan M. G. and Goeddel D. V. (1996) TRADD-TRAF2 and TRADD-FADD interactions define two distinct TNF receptor 1 signal transduction pathways. *Cell* **84**, 299–308.

Ichijo H., Nishida E., Irie K., ten Dijke P., Saitoh M., Moriguchi T., Takagi M., Matsumoto K., Miyazono K. and Gotoh Y. (1997) Induction of apoptosis by ASK1, a mammalian MAPKKK that activates SAPK/JNK and p38 signaling pathways. *Science* **275**, 90–94.

Kamata H., Honda S., Maeda S., Chang L., Hirata H. and Karin M. (2005) Reactive oxygen species promote TNFalpha-induced death and sustained JNK activation by inhibiting MAP kinase phosphatases. *Cell* **120**, 649–661.

Kang C. S., Zhang Z. Y., Jia Z. F., Wang G. X., Qiu M. Z., Zhou H. X., Yu S. Z., Chang J., Jiang H. and Pu P. Y. (2006) Suppression of EGFR expression by antisense or small interference RNA inhibits U251 glioma cell growth in vitro and in vivo. *Cancer Gene Ther.* **13**, 530–538.

Kaur R. and Vrati S. (2003) Development of a recombinant vaccine against Japanese encephalitis. *J. Neurovirol.* **9**, 421–431.

Krady J. K., Basu A., Allen C. M., Xu Y., LaNoue K. F., Gardner T. W. and Levison S. W. (2005) Minocycline reduces proinflammatory cytokine expression, microglial activation, and caspase-3 activation in a rodent model of diabetic retinopathy. *Diabetes* **54**, 1559–1565.

Liao C. L., Lin Y. L., Wang J. J., Huang Y. L., Yeh C. T., Ma S. H. and Chen L. K. (1997) Effect of enforced expression of human bcl-2 on Japanese encephalitis virus-induced apoptosis in cultured cells. *J. Virol.* **71**, 5963–5971.

Lin R. J., Liao C. L. and Lin Y. L. (2004) Replication-incompetent virions of Japanese encephalitis virus trigger neuronal cell death by oxidative stress in a culture system. *J. Gen. Virol.* **85**, 521–533.

Liu Z. G., Hsu H., Goeddel D. V. and Karin M. (1996) Dissection of TNF receptor 1 effector functions: JNK activation is not linked to apoptosis while NF-kappaB activation prevents cell death. *Cell* **87**, 565–576.

Mackenzie J. S., Johansen C. A., Ritchie S. A., van den Hurk A. F. and Hall R. A. (2002) Japanese encephalitis as an emerging virus: the emergence and spread of Japanese encephalitis virus in Australasia. *Curr. Top. Microbiol. Immunol.* **267**, 49–73.

Maggirwar S. B., Tong N., Ramirez S., Gelbard H. A. and Dewhurst S. (1999) HIV-1 Tat-mediated activation of glycogen synthase kinase-3beta contributes to Tat-mediated neurotoxicity. *J. Neurochem.* **73**, 578–586.

Maundrell K., Antonsson B., Magnenat E. *et al.* (1997) Bcl-2 undergoes phosphorylation by c-Jun N-terminal kinase/stress-activated protein kinases in the presence of the constitutively active GTP-binding protein Rac1. *J. Biol. Chem.* **272**, 25238–25242.

Mishra M. K., Koli P., Bhowmick S. and Basu A. (2007) Neuroprotection conferred by astrocytes is insufficient to protect animals

from succumbing to Japanese encephalitis. *Neurochem. Int.* **50**, 764–773.

Ohtsuka T., Buchsbaum D., Oliver P., Makhija S., Kimberly R. and Zhou T. (2003) Synergistic induction of tumor cell apoptosis by death receptor antibody and chemotherapy agent through JNK/p38 and mitochondrial death pathway. *Oncogene* **22**, 2034–2044.

Parquet M. C., Kumatori A., Hasebe F., Mathenge E. G. and Morita K. (2002) St. Louis encephalitis virus induced pathology in cultured cells. *Arch. Virol.* **147**, 1105–1119.

Samuel M. A., Morrey J. D. and Diamond M. S. (2007) Caspase-3 dependent cell death of neurons contributes to the pathogenesis of West Nile virus encephalitis. *J. Virol.* **81**, 2614–2623.

Sarker K. P., Biswas K. K., Yamakuchi M., Lee K. Y., Hahiguchi T., Kracht M., Kitajima I. and Maruyama I. (2003) ASK1-p38 MAPK/ JNK signaling cascade mediates anandamide-induced PC12 cell death. *J. Neurochem.* **85**, 50–61.

Satriotomo I., Bowen K. K. and Vemuganti R. (2006) JAK2 and STAT3 activation contributes to neuronal damage following transient focal cerebral ischemia. *J. Neurochem.* **98**, 1353–1368.

Slee E. A., Adrain C. and Martin S. J. (2001) Executioner caspase-3, -6, and -7 perform distinct, non-redundant roles during the demolition phase of apoptosis. *J. Biol. Chem.* **276**, 7320–7326.

Su H. L., Liao C. L. and Lin Y. L. (2002) Japanese encephalitis virus infection initiates endoplasmic reticulum stress and an unfolded protein response. *J. Virol.* **76**, 4162–4171.

Yang K. D., Yeh W. T., Chen R. F., Chuon H. L., Tsai H. P., Yao C. W. and Shaio M. F. (2004) A model to study neurotropism and persistency of Japanese encephalitis virus infection in human neuroblastoma cells and leukocytes. *J. Gen. Virol.* **85**, 635–642.

Yasui K. (2002) Neuropathogenesis of Japanese encephalitis virus. *J. Neurovirol.* **8**(Suppl. 2), 112–114.

Yoshizumi M., Abe J., Haendeler J., Huang Q. and Berk B. C. (2000) Src and Cas mediate JNK activation but not ERK1/2 and p38 kinases by reactive oxygen species. *J. Biol. Chem.* **275**, 11706–11712.

Zheng L., Bidere N., Staudt D., Cubre A., Orenstein J., Chan F. K. and Lenardo M. (2006) Competitive control of independent programs of tumor necrosis factor receptor-induced cell death by TRADD and RIP1. *Mol. Cell. Biol.* **26**, 3505–3513.

Zhu N., Khoshnan A., Schneider R., Matsumoto M., Dennert G., Ware C. and Lai M. M. (1998) Hepatitis C virus core protein binds to the cytoplasmic domain of tumor necrosis factor (TNF) receptor 1 and enhances TNF-induced apoptosis. *J. Virol.* **72**, 3691–3697.